Available online at www.sciencedirect.com
SCIENCE DIRECT®
European Journal of Pharmacology 479 (2003) 3–12
www.elsevier.com/locate/ejphar

Probing conformational changes in neurotransmitter transporters: a structural context

Naomi R. Goldberg[a], Thijs Beuming[b], Orkun S. Soyer[c], Richard A. Goldstein[c,d], Harel Weinstein[b,e], Jonathan A. Javitch[a,*]

[a] Center for Molecular Recognition, Columbia University, P&S 11-401, Box 7, 630 West 168th Street, New York, NY 10032, USA
[b] Department of Physiology and Biophysics, Mount Sinai School of Medicine, One Gustave Levy Place, New York, NY 10029, USA
[c] Department of Chemistry, University of Michigan, Ann Arbor, MI 48109, USA
[d] Division of Mathematical Biology, National Institute for Medical Research, The Ridgeway, Mill Hill, London NW7 1AA, UK
[e] Department of Physiology and Biophysics, Weill College of Medicine of Cornell University, 1300 York Avenue, New York, NY 10021, USA

Accepted 21 August 2003

Abstract

The Na^+/Cl^--dependent neurotransmitter transporters, a family of proteins responsible for the reuptake of neurotransmitters and other small molecules from the synaptic cleft, have been the focus of intensive research in recent years. The biogenic amine transporters, a subset of this larger family, are especially intriguing as they are the targets for many psychoactive compounds, including cocaine and amphetamines, as well as many antidepressants. In the absence of a high-resolution structure for any transporter in this family, research into the structure–function relationships of these transporters has relied on analysis of the effects of site-directed mutagenesis as well as of chemical modification of reactive residues. The aim of this review is to establish a structural context for the experimental study of these transporters through various computational approaches and to highlight what is known about the conformational changes associated with function in these transporters. We also present a novel numbering scheme to assist in the comparison of aligned positions between sequences of the neurotransmitter transporter family, a comparison that will be of increasing importance as additional experimental data is amassed.

Keywords: Conformational change; Neurotransmitter transporter; Structural context

1. Introduction

The Na^+/Cl^--dependent neurotransmitter transporters constitute a family of homologous membrane proteins responsible for the reuptake, from the synaptic cleft, of neurotransmitters including dopamine, serotonin (5-HT), norepinephrine, γ-aminobutyric acid (GABA), and glycine as well as other small molecules such as proline, creatine, betaine, and taurine. This family has been designated the neurotransmitter:sodium symporter (NSS) family 2.A.22 by Saier (Saier, 1999). These transporters couple the movement of Na^+ down its electrochemical gradient to the translocation of substrate across the plasma membrane. The biogenic amine transporters, including the dopamine transporter (DAT), norepinephrine transporter (NET), and the serotonin transporter (SERT), are the molecular targets for psychostimulant drugs, such as cocaine and amphetamine, and for many antidepressants.

The absence of a high resolution structure for any member of this family limits current understanding of the relationship between the molecular structure and the functional mechanisms of these transporters. As reviewed recently, insights into structure–function properties of the transporters have emerged from analysis of the effects of site-directed mutations and chimeras (Chen and Reith, 2002; Goldberg et al., 2003; Norregaard and Gether, 2001). Here we review current knowledge of the conformational changes associated with their binding and transport functions. To aid in the comparative analysis across families of transporters in different species, we employ a novel generic numbering scheme that enables the comparison of aligned positions within the sequences of the members of the NSS family (Goldberg et al., 2003) and we summarize computational

* Corresponding author. Tel.: +1-212-305-7308; fax: +1-212-305-5594.
E-mail address: jaj2@columbia.edu (J.A. Javitch).

0014-2999/$ - see front matter © 2003 Elsevier B.V. All rights reserved.
doi:10.1016/j.ejphar.2003.08.052

analyses that help us to infer the secondary structure and orientation of the transmembrane segments.

2. Generic numbering scheme

We have developed a common residue numbering scheme that facilitates comparison of the sequences of different NSSs (Goldberg et al., 2003). The numbering scheme is informative of the relative position of each amino acid, the amino acid present at that position and the actual amino acid number in a particular transporter. Each generic residue number starts with the index of the transmembrane segment (TM), e.g. 1 for TM1, and is followed by a number indicating the position of the residue in the sequence, relative to a reference residue that is the most conserved position in that TM. The reference residue is arbitrarily assigned the number 50. For example, as our reference residue in TM1 we chose, in the manner described below, a tryptophan, the generic number of which would be 1.50, i.e. $Trp_{1.50}$. When referring to a particular transporter, the generic number can be preceded by the number of the residue in the particular sequence. In the human dopamine transporter (hDAT), this tryptophan in TM1 is at position 84, so this residue is referred to as $Trp84_{1.50}$. A serine residue located five amino acids C-terminal to $Trp84_{1.50}$ is designated $Ser89_{1.55}$. A similar numbering scheme had been developed for G-protein-coupled receptors (Ballesteros and Weinstein, 1995).

The conserved residues identified as 50 were chosen from a sequence alignment analysis. There are more than 100 residues among a set of 52 mammalian Na^+-dependent NSSs of known function that are 100% conserved (alignment not shown). To decide which residue is the most appropriate reference residue for each of the TMs, we searched for additional sequences with similarity to the mammalian NSSs, and investigated the decrease in conservation for alignments of increasing size.

Blasting the Swissprot and TrEMBL databases with several query NSS sequences yielded 291 hits with e-values <0.001. (No fragments were included in the alignment.) These included 120 mammalian proteins (of which 38 are orphans), 42 drosophila proteins (of which 38 are orphans), 17 proteins from *C. elegans* (of which 15 are orphans), 72 bacterial proteins, 14 archaeal proteins, and 26 proteins from other species. Among these bacterial and archaeal proteins, only the function of TnaT has been identified; this protein is a Na^+-dependent tryptophan transporter from *Symbiobacterium thermophilum* (Androutsellis-Theotokis et al., 2003).

The sequence alignment was ranked in terms of similarity to the original set of 52 mammalian transporters. Each of the 291 sequences was aligned individually against each of the 52 mammalian transporters, and the average similarity (% identity) was taken as a measure of the similarity of that sequence to the group of mammalian transporters. Multiple alignments were generated with gradually decreasing average sequence identity. The alignments included all sequences with average identity >45% (100 sequences, including all mammalian NSSs), 35% (133 sequences), 30% (174 sequences), and 20% (260 sequences), respectively. Based on these alignments, we have selected the most appropriate 'reference residue' in each TM based on the extent of conservation in as large an alignment as possible, with the additional criterion that it is located within the putative transmembrane segment (see below). The 12 amino acids chosen as reference residues are shown in Table 1 and are indicated by blue circles in Figs. 1–3.

Table 1

TM	Index number	Reference residue in hDAT	Conservation in all 133 sequences with >35% identity (%)	Conservation in all 291 sequences (%)
1	1.50	W84	99	91
2	2.50	P112	99	89
3	3.50	Y156	98	91
4	4.50	C243	81	50
5	5.50	L287	98	83
6	6.50	Q317	100	93
7	7.50	F365	100	85
8	8.50	F412	100	86
9	9.50	G468	100	95
10	10.50	G500	100	75
11	11.50	P529	100	71
12	12.50	G561	98	78

All 12 reference residues are 100% conserved in the mammalian NSSs, and all are highly conserved in the sequences that are assumed to produce a similar structural framework (i.e. identity>20%). (Although $Cys_{4.50}$ is 83% conserved in the 100 sequences with greater than 45% sequence identity, threonine is present in another 15% of these sequences, for a total conservation of 98%.) Most reference residues have a high degree of conservation in the alignment including all sequences with identity >20%, except for $Cys/Thr_{4.50}$, which is only conserved among all sequences with identity >25% (but which is nonetheless the most conserved residue in TM4 in the larger alignments). For the larger alignments ($\leq 20\%$ average identity), a number of sequences contain insertions and deletions in TM9 and TM10, in particular at positions $Gly_{9.50}$ and $Gly_{10.50}$. The significance of these structural differences is unclear, and it is not yet known whether these proteins are functional.

3. Secondary structure prediction of Na^+/Cl^--coupled neurotransmitter transporters

To develop a structural context for the management of structure–function data, we have developed a prediction of the secondary structure parsing of this transporter family, based on approaches and algorithms that have served in the study of other families of membrane proteins (e.g. the G

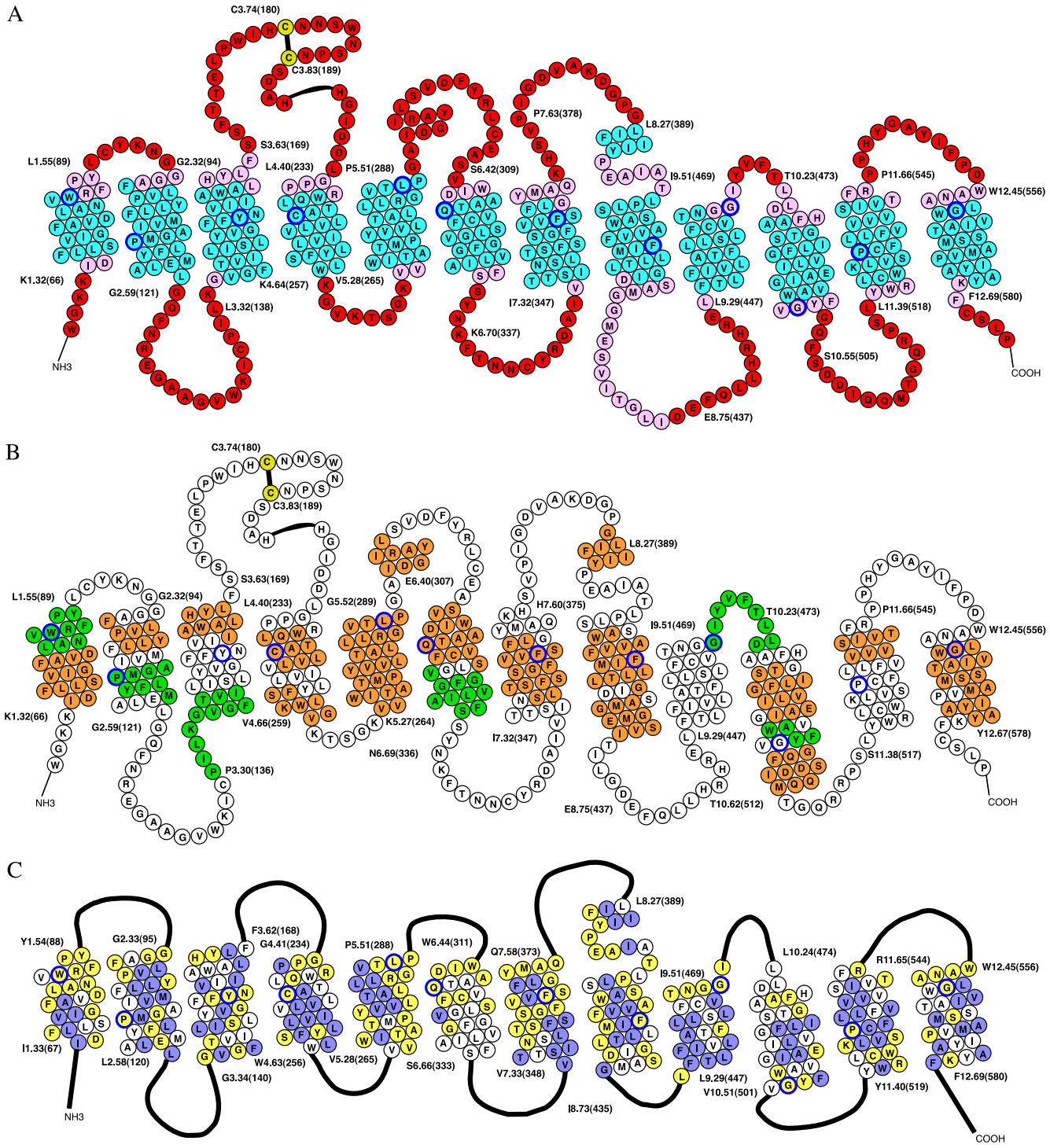

Fig. 1. Predicted structural properties of neurotransmitter transporters. The helical nets represent the human dopamine transporter, with the single letter code of each amino acid within a circle. The most conserved residues in the twelve transmembrane segments (index number TM#.50—see text) are identified by thick blue lines surrounding the circles. The index numbers are shown for selected residues, with human DAT residue numbers in parentheses. In (A) and (B), cysteines in the second extracellular loop thought to form a disulfide bond are shown in yellow. When not shown, residues in the N- and C-termini and in loops are indicated by black lines. (A) *Predicted transmembrane topology.* Based on hydrophobicity analysis, residues in cyan are predicted to be located within the lipid bilayer, and residues in red are predicted to be solvent exposed outside the lipid boundaries. Regions that are not well defined by the prediction methods are shown in pink. The assignment of residues to the transmembrane segment is based on the hydrophobicity analysis as well as on predictions of secondary structure, lipid accessibility and the summarized experimental data, all of which are discussed below and in the text. (B) *Secondary structure propensity based on the spatial periodicity of residue properties*. Predicted α-helical segments are shown in orange; sequential residues with periodicity consistent with β-strand are shown in green. Segments shown in white did not exhibit an identifiable periodicity. (C) *Probability of lipid exposure*. Positions shown in blue are predicted to lie on the helix-lipid interface, positions in yellow are predicted to face the protein interior, and white regions are undefined (see text).

protein-coupled receptors (Ballesteros and Weinstein, 1995; Visiers et al., 2002)). The methods have been collected in a suite of programs named ProperTM (http://icb.med.cornell.edu/services/propertm/start). This suite of programs allows for user driven sequential applications of various algorithms that have been applied broadly and, in selected cases, have been validated by subsequent determined structures (for reviews, see Ballesteros and Weinstein, 1995; Visiers et al., 2002). In brief, the algorithms encode prediction methods based on the calculation of position-associated properties (hydrophobicity, volume, conservation) identified in a multiple sequence alignment. The prediction of secondary structure and of the residues facing protein (inward) or lipid (outward) is based on the analysis of this information. The methods in ProperTM have been designed to analyze membrane proteins, but some of the applications (e.g. the calculation of a conservation index) are generally applicable. The representations of the structural features in the annotated helical nets in Fig. 1 display information obtained with the ProperTM suite of programs calculated from the alignment of NSS sequences. The structural characteristics of the transporters summarized in the figures include the following subsections.

3.1. Hydrophobicity

The parsing of the transporter sequences into the TM domains has been determined using three different methods. Average *hydrophobicity* was calculated with ProperTM using different window-sizes and the Kyte and Doolittle scale (Kyte and Doolittle, 1982), and TM segments were identified as regions with high overall hydrophobic character. Additionally, TM domains were predicted with TMHMM, a hidden Markov model based approach (Krogh et al., 2001) and PHDHTM, a profile based neural network method (Rost et al., 1995). The hydrophobic segments in Fig. 1A represent the consensus result of these three different methods.

3.2. Secondary-structure propensity

A central element in the prediction of *secondary structure* is the periodicity of sequence conservation, which has proven to be a good indicator in a number of membrane proteins (Donnelly et al., 1993). The periodicity is quantified with Fourier transform (FT) analysis, in which a property profile is calculated over a window size N to produce a power spectrum $P(\omega)$ for the entire sequence. A peak in the power spectrum around 105°, the angle between adjacent side-chains in an α-helix viewed down its axis, indicates that the sequence contained within the window N adopts α-helical conformation. For beta strands, the peak should appear between 166° and 180°. The periodicity of a given property (e.g., hydrophobicity) calculated from $P(\omega)$ for α-helical and β-strand structures characterizes the relative extent of periodicity in the α-helical/β-strand region

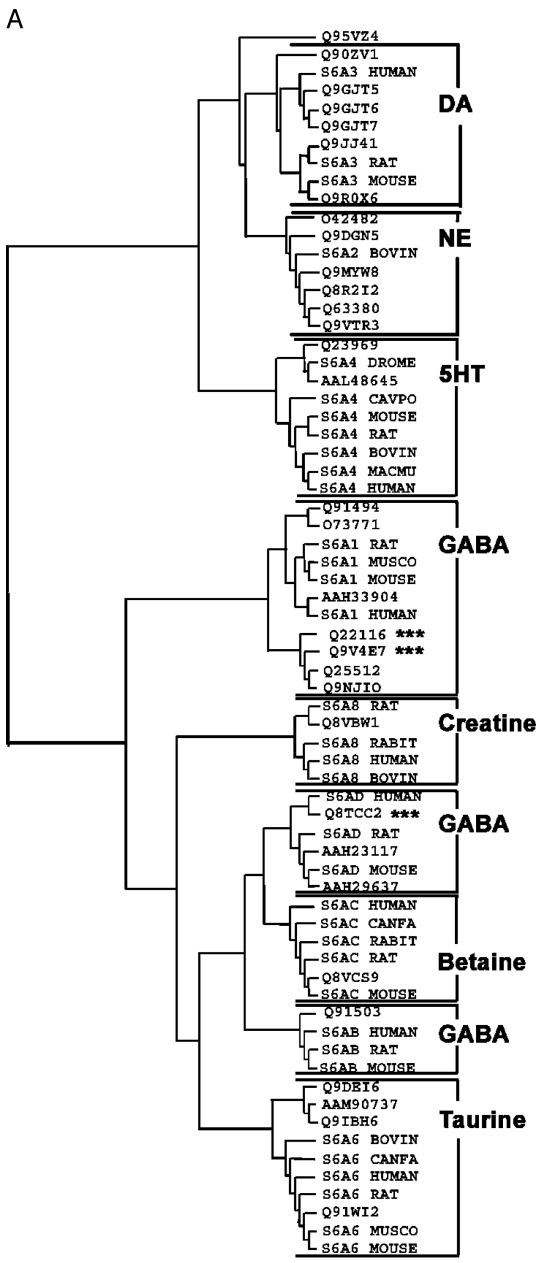

Fig. 2. Phylogenetic tree and predictions of the evolutionary model. (A) Phylogenetic tree of transporter proteins that were used to create the evolutionary model. This is a consensus tree from 2000 trees sampled during a Markov Chain Monte Carlo run, using Mr. Bayes, a state-of-the-art tree inference software (Huelsenbeck and Ronquist, 2001). The tree is rooted at the midpoint of the longest branch. Transporters forming a monophyletic subfamily are indicated as, DA; dopamine transporters, NE; norepinephrine transporters, 5HT; serotonin Transporters, GABA, taurine, betaine, and creatine. The single sequence that does not fall under any of the subfamilies is an octopamine transporter from *trichoplusia ni* (cabbage looper) (SWISSPROT ID: Q95VZ4). Sequences at the end of branches indicated with 3 stars-Q22116, Q9V4E7, Q8TCC2-are orphan transporters from *C. elegans*, drosophila, and human, respectively. (B) Lipid/interior-facing location predictions based on 5-site class model derived from "30nf" alignment. Locations predicted to face the protein interior (probability of site classes 1 and 2 above 0.5) and lipid are colored yellow and blue, respectively. As explained in the text, "slow evolving" locations are assumed to face the protein interior.

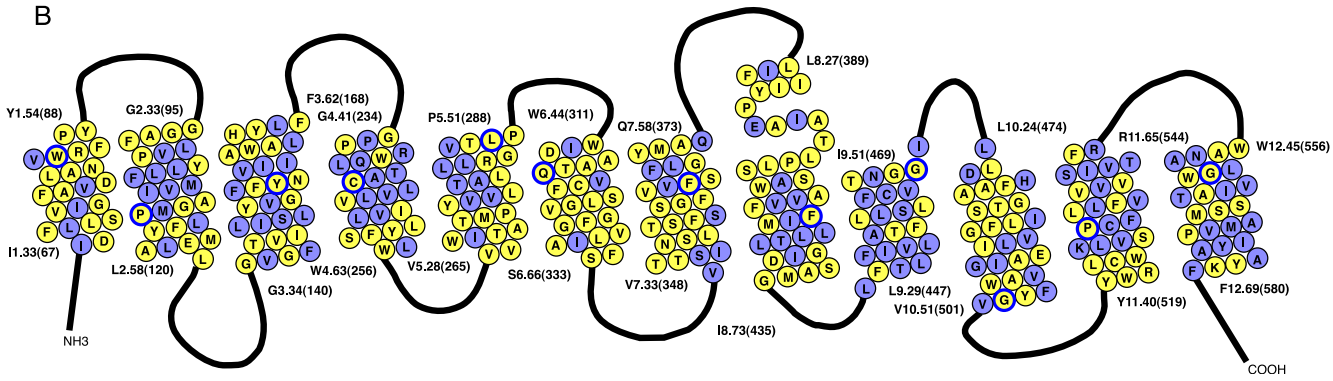

Fig. 2 (*continued*).

compared to the entire spectrum. Illustrations of these characteristics are shown in Fig. 1B.

3.3. Conservation and lipid-facing probability

An approach to the calculation of *conservation* at a given locus in the sequence has been proposed on the basis of the polytope-method and the information content analysis of the alignment (Shi et al., 2001; Visiers et al., 2002). In this approach, the degree of conservation at each position in the alignment is determined by (1) the number of different amino acids; (2) the probability of finding a particular residue replaced by another; and (3) the frequency of appearance of each type of residue. These factors are integrated to calculate the conservation index (CI).

Based on the assumed relation between the degree of conservation and the probability of a given locus to face inward (high conservation) or outward (low conservation), the CI can be used to predict the lipid facing residues in a TM. The prediction of *lipid-facing* sides of the TM segments was based on the analysis of properties of the individual residues in the context of the alignment. Thus, the lipid facing side of the TM was considered to include the positions with a low conservation index, high average hydrophobicity (hdp) and a low hydrophobicity standard deviation (σ_{hdp}). These factors were integrated within ProperTM to calculate the probability that an amino acid at a particular position lies on a protein–lipid interface. This method was tested on the known structure of the photo-reaction center and a multiple sequence alignment of 12 photo-reaction center sequences (Ballesteros et al., unpublished) and was found to be very discriminant when used with an appropriate threshold value. Lipid facing probabilities are shown in Fig. 1C. Note, however, that the strong dependence of the prediction of lipid-facing probability on the variability or CI-criterion may misidentify, as pointing

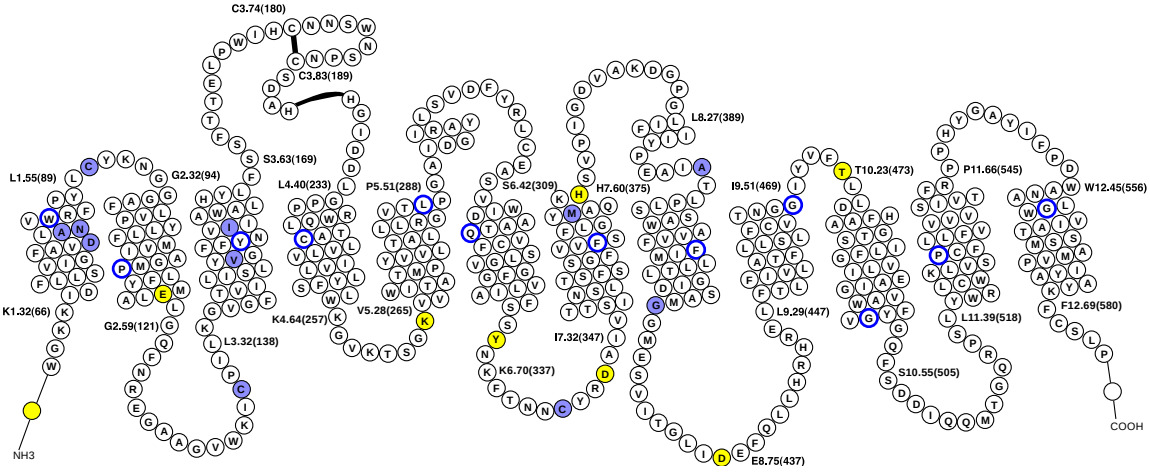

Fig. 3. Summary of experimental findings from the neurotransmitter transporter family. As in Fig. 1, the helical nets represent the human dopamine transporter, with the single letter code of each amino acid within a circle and with the index positions outlined in blue. Residues not shown in the N- and C-termini are indicated by black lines. Endogenous cysteines or substituted cysteines in DAT (or at the aligned positions in other NSSs) are shown in blue if they were found to be accessible to sulfhydryl reagents in a manner that was sensitive to the presence of substrate and/or inhibitor. Residues in DAT (or at the aligned positions in other NSSs) are shown in yellow if the mutation affected the accessibility of a conformationally sensitive residue or was inferred to alter the distribution of conformational states of the transporters.

outwards toward lipid, the inward-facing residues that are not conserved because of their involvement in subtype-selective functions. One possible example in the present case is the region in TM3 surrounding the conserved $Tyr_{3.50}$, in which non-conserved hydrophobic residues (e.g. $Val_{3.46}$) have been inferred to be involved in ligand binding (Chen et al., 1997).

4. Properties of the transporters predicted from evolution-based sequence analysis

The underpinning of all computational sequence analysis is that the proteins under study are evolutionarily related and therefore may share common structural and functional features, which might leave detectable patterns in their sequences. A proper representation of these evolutionary relationships is important in detecting and evaluating such patterns. Phylogenetic relationships can induce their own patterns, which can confound comparative sequence analysis, especially in the analysis of correlated changes (Pollock and Taylor, 1997). In addition, evolutionary distance is an important consideration when distinguishing between sequence similarities resulting from strong selective pressures and those resulting from inadequate divergence time. This is especially critical since more closely related proteins are more likely to share functional and structural characteristics. As a result, it can be difficult to unravel which patterns of conservation come from shared characteristics and which arise from the limited number of mutations that have occurred. It is difficult to evaluate the statistical significance of the observed patterns of conservation and variation without an underlying model that explicitly includes the evolutionary relationships between the sequences and the manner in which they change.

In general, the amount of evolutionary information that can be incorporated into a sequence analysis method is limited by the available evolutionary models. Current popular models of evolution (Felsenstein, 1981; Yang, 1993; Yang and Rannala, 1997) have primarily been developed for inferring phylogenetic relations among proteins and are of limited use in deriving functional or structural information. This limitation is mainly due to the use of a single substitution matrix to model evolution over the entire sequence of the protein. Recently, a novel evolutionary model has been developed (Dimmic et al., 2000; Koshi and Goldstein, 1998; Koshi et al., 1999; Soyer et al., 2002) to relax this limitation and allow different parts of the protein to be modeled by different substitution matrices. This model makes it possible to base the entire analysis on the modeling of the molecular evolution instead of ignoring or including such information as a secondary consideration, and can be used directly to gain functional and structural insights into the proteins under study.

In brief, the model relaxes the "one substitution matrix for all locations" approach of conventional evolutionary models. It allows for variation at different locations by postulating that each location in a set of aligned sequences can be described by one of a number of different *types* of sites, called "site classes," each associated with a specific substitution model. Neither the assignment of locations to different site classes nor the corresponding substitution models are known a priori. Rather, these models are optimized using a maximum likelihood formulation, given a multiple sequence alignment and associated phylogenetic tree. Once the substitution models have been derived, however, it is possible to assign the locations to different site classes a posteriori. This approach allows us to identify locations in the protein that are under similar selective pressure and to characterize the nature of these selective pressures as well as changes in these selective pressures, while avoiding unnecessary and potentially limiting assumptions about the causes underlying these differences.

This "hidden-sites" model allows a determination of the parameters for a limited number of site classes using all available sequence data. Even with this simplification, the limited amount of available sequence data makes it necessary to reduce the number of adjustable parameters used to describe the substitution rates for each site class. This is achieved by considering the relative "fitness" $F_k(A_i)$ of amino acid A_i for any location described by a particular site class k. The fitness value is related to the logarithm of the propensity of finding such an amino acid at any location described by this site class. Moreover, we assume that the probability of substitution between two amino acids should depend on the change in fitness values resulting from such a substitution. Thus, for each site class the matrix of all possible substitutions is based on the fitness values of the amino acids in that particular site class. In other words, the substitution rate between two given amino acids in a given site class can be calculated using the difference of fitness values of these amino acids in that site class.

A phylogenetic tree (Fig. 2A) was created using the alignment described above containing all transporters with greater than 30% identity. This tree indicates a clear subfamily structure to NSSs, with GABA, taurine, creatine, and betaine transporters closely related to each other and separated from transporters for serotonin, norepinephrine, and dopamine. A 5-site class evolutionary model was optimized based on this phylogenetic relation. Table 2 lists the evolutionary rate and the correlation values between fitness values and physicochemical properties of amino acids for each of the site classes in this model. Site classes 2 and 3 showed very similar correlations among fitness and physical property values of amino acids. Both sets of correlations suggest that these site classes comprise locations that are selected for their hydrophobicity and membrane preferences, suggesting that locations in the transmembrane domain are assigned primarily to these two site classes. A further inference from these data is that among these locations, those that face the lipid and that have relatively more freedom in accommodating different residues are assigned

Table 2
Summary of the 5-site class model derived using the "30nf" alignment and the associated phylogenetic tree (see text)

Site class	Subst. rate	Top 4 distinct correlations	
		CC	Property
1	0.031	− 0.49	Side Chain Width (FAUJ880105)
		− 0.43	Helix Freq. (TANS770102)
		− 0.52	Relative Mutability (JOND920102)
		− 0.39	Positive Charge (FAUJ88011)
2	0.187	− 0.79	Accessible Area (JANJ780101)
		− 0.78	Exposed % (JANJ780103)
		− 0.77	Polarity (ZIMJ680103)
		0.75	Interactions per side chain atom (WARP780101)
3	0.491	0.78	Hydopathy (KYTJ820101)
		0.73	Membrane Preference (DESM900101)
		0.69	Inner Beta Sheet Probability (KANM800104)
		0.67	Hydration Potential (WOLR810101)
4	0.981	− 0.92	Hydrophobicity (CIDH920102)
		0.90	Flexible (VINM940102)
		− 0.90	Lipid to Surface Energy (WIMW960101)
		0.89	Polarity (GRAR740102)
5	2.130	− 0.75	Charge Donor Capacitiy (CHAM830108)
		− 0.75	Principal Property z2 (WOLS870102)
		0.73	Transfer Energy from Vapor to Chx. (RADA880103)
		− 0.65	Absolute Entropy (HUTJ700102)

Subst. rate is the substitution rate. CC is the correlation coefficient. The top four distinct correlations among fitness values for each site class and the physical properties of the amino acids are listed. The codes in parentheses are those from AAindex_v03 database (Kawashima et al., 1999).

to site class 3 (faster evolving than site class 2), whereas those that face the protein interior and are more restricted are assigned to site classes 1 and 2 (slowly evolving). We expect that locations towards the ends of TM helices will be assigned primarily to site classes 4 and higher, which have faster rates of evolution and show high correlation with flexibility and accessibility. These inferences are based in part on a recent study of G-protein-coupled receptor sequences, in which the resulting 5-site class evolutionary model showed very similar properties to the one presented here (Soyer et al., submitted for publication).

The 5-site class model was used to predict the orientation of transmembrane locations with respect to the lipid bilayer, by assigning all putative transmembrane locations that have a combined posterior probability of 0.5 or higher for site classes 1 and 2 as facing the protein interior. All remaining transmembrane locations were assigned as facing the lipid or solvent (Fig. 2B). For 81% of transmembrane locations, predictions from the evolutionary model match those of the methods described above (compare Figs. 1C and 2B). The success of such methods, based on the properties observed from sequence alignments, in predicting the structure of G protein-coupled receptors is evidenced by the agreement with the structural properties observable in the crystal structure of rhodopsin. This success suggests that the combined predictions illustrated here provide the best available inferences about the orientation of transmembrane locations with respect to the lipid bilayer in the NSS family members.

The evolutionary model is mainly designed to detect the different selective pressures acting on a given set of proteins and group locations that are under similar selective pressures. Although this model can lead to several functional/structural inferences about the proteins under study, it is not designed to test specific a priori predictions. It may be possible, however, to improve the accuracy of inferences by optimizing the model towards detecting a particular feature of interest. We are currently further analyzing the site-classes in this and higher site class models in an attempt to correlate the classes with other structural and functional elements of the NSSs. For example, in the 5-site class model, site classes 4 and 5 have higher rates of evolution, and their fitness values show higher correlations to properties such as hydophilicity, polarity, and solvent exposure. These site classes mostly comprise the loop regions, and additional analyses may allow a differentiation of site classes in these regions that correlate with different functions, such as conformational change associated with transport.

5. Conformational changes associated with transport

Conformational changes associated with transport have been identified in both intracellular and extracellular loops as well as in transmembrane regions. Given the limited amounts of these transporters that are available for analysis, nearly all studies have relied upon indirect determinations of conformational change. Reaction of an endogenous or substituted cysteine with a sulfhydryl reagent may be sensitive to the presence of substrates, neurotransmitters and/or co-transported ions, through direct steric protection or by inducing or stabilizing a conformational change that makes the cysteine less accessible to reaction. In DAT, for example, cocaine significantly retarded the reaction of methanethiosulfonate (MTS) reagents with $Cys135_{3.29}$ in intracellular loop 1, and $Cys342_{6.75}$ in intracellular loop 3 (Ferrer and Javitch, 1998). Since mutation of these cysteines had no effect on cocaine's affinity for DAT, the protection most likely results from a cocaine-induced conformational change that reduces the accessibility of the cytoplasmic loop cysteines. Inward transport of the substrate, *m*-tyramine, enhanced the MTS ethylammonium (MTSEA)-induced inactivation of dopamine uptake at $Cys342_{6.75}$ (Chen et al., 2000). This effect of tyramine was temperature sensitive and was Na^+-dependent, suggesting that tyramine exposes $Cys342_{6.75}$ during translocation, rather than simply by binding. Moreover, cocaine protected against tyramine's effect at $Cys342_{6.75}$, presumably by blocking transport and preventing exposure of this endogenous cysteine.

The corresponding position in SERT, $Cys357_{6.75}$, is also conformationally sensitive; the ability of 5-HT and cocaine

to protect this site from MTSEA-induced inactivation presumably required a conformational change, as it was Na^+- and temperature-dependent (Androutsellis-Theotokis et al., 2001). Moreover, reaction of $Cys357_{6.75}$ with MTSEA was increased in the presence of alkali cations, particularly K^+, suggesting that the accessibility of $Cys357_{6.75}$ varies with the conformation of the transporter. Consistent with a role of intracellular loop 3 in conformational change, $Tyr335_{6.68}$ in DAT appears to play a role in regulating the distribution between different conformational states of the transport cycle (Loland et al., 2002). Mutation of this residue to alanine caused conversion of the endogenous inhibitory Zn^{2+} switch to an activating one, in which binding of Zn^{2+} to inactive mutant transporter leads to uptake. The explanation offered for this observation was that mutation of $Tyr335_{6.68}$ alters the conformational equilibrium of the translocation cycle, with accumulation in conformational states following substrate binding, and that Zn^{2+} is able to reverse this change. The dramatic decrease (up to 150-fold) in affinity of $Y335_{6.68}A$ for cocaine-like inhibitors and the increased apparent affinity for substrates, is consistent with an altered conformational equilibrium.

The accessibility to MTS reagents of $Cys399_{8.63}$ in intracellular loop 4 of the GABA transporter (GAT) is dependent on transporter conformation (Golovanevsky and Kanner, 1999). In WT GAT-1, but not the $C399_{8.63}S$ mutant, binding of both Na^+ and Cl^-, as well as the nontransported GABA analogue, SKF100330A, reduced the sensitivity to sulfhydryl modification; in contrast, GABA, in the presence of NaCl, increased the reactivity to MTS reagents. Finally, mutation of $Arg44_{1.26}$ in the cytoplasmic N-terminus of GAT was inferred to impair the reorientation of unloaded transporter after the release of substrate to the intracellular medium (Bennett et al., 2000).

Cocaine increased the rate of reaction of $Cys90_{1.56}$ in EL1 with MTS reagents, presumably by triggering a conformational change that increased the accessibility of this extracellular cysteine (Ferrer and Javitch, 1998). However, the DAT inhibitors benztropine and cocaine had different effects on the reaction of the extracellular $Cys90_{1.56}$ and the intracellular $Cys135_{3.29}$ (Reith et al., 2001): benztropine did not protect $Cys135_{3.29}$ in intracellular loop 1 from MTS ethyltrimethylammonium (MTSET) inactivation, and also did not increase the reaction of $Cys90_{1.56}$ with MTSET. This finding suggests that inhibitors do not all stabilize the same conformational state. The same type of reactivity studies suggest that EL1 is also subject to ion-induced conformational changes: lithium caused a change in SERT $Cys109_{1.56}$ reactivity as well as cocaine binding and ion conductance (Ni et al., 2001), whereas Na^+ and Cl^- protected against MTSET inactivation at a cysteine inserted at position 1.56 in GLYT2, in a temperature-dependent manner (Lopez-Corcuera et al., 2001).

A chimeric transporter, in which a short stretch of NET was substituted into the first half of EL2 in SERT, was substantially impaired for serotonin transport (< 10% WT SERT), whereas antagonist and substrate binding and surface expression were intact (Stephan et al., 1997). Chimeras in which the extracellular loops of SERT were replaced, one by one, with the corresponding sequence from NET, expressed and had normal SERT antagonist selectivity. In contrast, the EL4, EL5, and EL6 chimeras had dramatically impaired transport (Smicun et al., 1999). GAT EL4, EL5, and EL6 have been proposed to contribute to the substrate binding site, based on work that swapped external sequences between various GAT isoforms (Tamura et al., 1995). Substitution of three residues from EL5 of GAT-1 with the aligned residues in GAT-2, GAT-3, and GAT-4, imparted to GAT-1 sensitivity to β-alanine inhibition of GABA uptake, as seen with GAT-2, 3, and 4. Furthermore, Cao and coworkers used hSERT-rSERT chimeras and point mutations to identify position $490_{10.23}$ and neighboring residues in EL5, as determinants of the difference in pH dependence of transport-associated currents between the hSERT and rSERT (Cao et al., 1998). This region was inferred to participate in the external gating of SERT. The mutation $K448_{10.23}E$, in EL5 of GAT, was also shown to confer pH sensitivity and alter substrate interactions of the transporter (Forlani et al., 2001).

In rGAT, mutation of $Met345_{7.56}$ or $Thr349_{7.60}$ to histidine altered the affinity for the substrates GABA and Na^+. In addition, the mutations differentially shifted the charge/voltage relationships and the lithium-induced leak currents, suggesting a role for the extracellular end of TM7 in regulating the distribution of conformational states of the transport cycle (MacAulay et al., 2003).

At the extracellular ends of TM7 and TM8 in DAT, treatment of $M371_{7.56}C$ and $A399_{8.37}C$ with MTSET inhibited dopamine uptake (Norregaard et al., 2003). Inactivation of $M371_{7.56}C$ was enhanced by Na^+ and prevented by dopamine in a Na^+-dependent manner. Since dopamine binding is believed to be Na^+-independent, this suggests that dopamine induces a transport-associated conformational change that decreases the reactivity of $M371_{7.56}C$ with MTSET. In contrast, cocaine inhibited the reaction of $A399_{8.37}C$ with MTSET, either directly or indirectly, whereas dopamine had no effect.

In the transmembrane domain, cysteines substituted for $Asp98_{1.45}$, $Gly100_{1.47}$, and $Asn101_{1.48}$ rendered hSERT sensitive to inhibition by MTSET with protection by 5-HT and/or cocaine (Henry et al., 2003). These findings suggest a possible contribution of these residues in TM1 to the substrate binding pocket, but it is also conceivable that this effect was indirect and resulted from conformational rearrangement. In addition, in SERT, protection by 5-HT from inactivation by MTSET at 3.46 was both temperature- and Na^+-independent, and therefore also inferred to result from direct steric block and not a conformational change (Chen and Rudnick, 2000). Cysteine substituted for $Ile172_{3.46}$ was accessible to both external and cytoplasmic reagents (Chen and Rudnick, 2000), suggesting that this position may form a part of the substrate binding site that is alternately exposed

to the extracellular and intracellular milieu, consistent with an alternate access model of transport (Hilgemann and Lu, 1999).

Reaction of SERT I179$_{3.53}$C with MTSET inactivated transport but not binding (Chen et al., 1997). Neither cocaine nor 5-HT protected against reaction with MTSET. These observations suggest that Ile179$_{3.53}$ is not associated with the binding site, but may be involved with some conformational event subsequent to substrate binding. Na^+ enhanced the inactivation of Ile179$_{3.53}$C, as well as stimulated its reactivation by free cysteine, an effect that was enhanced by the presence of 5-HT (Chen and Rudnick, 2000). These results suggest that since 5-HT can bind the inactivated Ile179$_{3.53}$, the transporter is locked in an outward facing form, and that Ile179$_{3.53}$ exists in a part of the transporter that changes conformation upon binding of Na^+ and 5-HT. In NET, MTSET inactivation of I155$_{3.53}$C was enhanced by cocaine but slowed by dopamine, presumably by transport-associated occlusion of 155$_{3.53}$. Thus, this region of the transporter has been proposed to form part of an extracellular gate, which is normally sequestered upon substrate translocation, and which is prevented from closing upon cysteine modification.

The accessibility of I159$_{3.53}$C in DAT has been used recently as a conformational sensor for probing the effects of intracellular loop mutations. As for DAT Y335$_{6.68}$A, mutation to alanine of three additional intracellular positions, Lys264$_{5.27}$, Asp345$_{7.30}$, and Asp436$_{8.74}$, produced diminished uptake which was potentiated by Zn^{2+} and decreased the affinity for cocaine and other inhibitors (Loland et al., submitted). The conformational state of K264$_{5.27}$A, Y335$_{6.68}$A, and D345$_{7.30}$A was investigated by assessing the accessibility to MTSET of I159$_{3.53}$C in an MTSET-insensitive 'E2C' background (C90$_{1.56}$A/C306$_{6.39}$A). Unlike its effect at the corresponding position in NET (I155$_{3.53}$C), MTSET did not inhibit uptake mediated by E2C-I159$_{3.53}$C in the presence or absence of dopamine, cocaine or Zn^{2+}. In this background, the mutants K264$_{5.27}$A, Y335$_{6.68}$A and D345$_{7.30}$A were also not inactivated by MTSET; in the presence of 10 μM Zn^{2+}, however, MTSET inhibited uptake. As in NET I155$_{3.53}$C, this inhibition was protected by dopamine and enhanced by cocaine. These data are consistent with the model proposed above in which Zn^{2+} partially reverses an altered conformational equilibrium in the cytoplasmic loop mutant transporters. They also suggest that the conformational equilibrium produced by the mutations resembles that of the NET more than that of the DAT.

Glu101$_{2.55}$, at the intracellular end of TM2 in GAT, was inferred to be critical for the conformational changes GAT undergoes during its transport cycle (Keshet et al., 1995). Mutation of Glu101$_{2.55}$ to aspartate or other residues abolished transport despite unaltered surface expression. The transient Na^+ currents observed in WT, thought to represent Na^+ binding to the transporter and/or conformational changes in response to Na^+ binding, were not observed in these mutants. Thus, a defect in the binding or unbinding of Na^+ may result from mutation of Glu101$_{2.55}$.

6. Conclusions

The work reviewed here indicates that even in the absence of a high resolution structure of any transporter in the NSS family, it is possible to apply comparative methods of structure analysis to obtain insight about the structural context of function in this class of membrane proteins. The studies reviewed suggest that cocaine and related uptake inhibitors are not merely neutral blockers but themselves induce conformational changes in the transporters to which they bind. Many mutations of DAT appear to affect cocaine binding indirectly by altering the distribution of conformational states of the transporter, in a way analogous to constitutive-activation of G protein-coupled receptors. Moreover, the loop regions have been widely implicated in conformational change in various NSSs, consistent with a model in which intracellular and extracellular loops form "gates" that alternately block and expose a substrate pathway to the extracellular and intracellular milieu. The recent identification of the bacterial and archaeal transporters and their potential suitability for direct structural studies raise the exciting prospect of being able to test specific structural hypotheses related to transport suggested by the studies. To facilitate such cross-species investigations of structure–function relations, we have presented here a generic numbering scheme in a context of predicted structural properties.

Acknowledgements

This work was supported in part by National Institutes of Health Grants DA12408, DA11495, MH57324, DA00060, and LM0577, the Lebovitz Fund, and the University of Michigan Bioinformatics Department.

References

Androutsellis-Theotokis, A., Ghassemi, F., Rudnick, G., 2001. A conformationally sensitive residue on the cytoplasmic surface of serotonin transporter. J. Biol. Chem. 276, 45933–45938.

Androutsellis-Theotokis, A., Goldberg, N.R., Ueda, K., Beppu, T., Beckman, M.L., Das, S., Javitch, J.A., Rudnick, G., 2003. Characterization of a functional bacterial homologue of sodium-dependent neurotransmitter transporters. J. Biol. Chem. 278, 12703–12709.

Ballesteros, J., Weinstein, H., 1995. Integrated methods for the construction of three-dimensional models of structure–function relations in G protein-coupled receptors. Methods Neurosci. 25, 366–428.

Bennett, E.R., Su, H., Kanner, B.I., 2000. Mutation of arginine 44 of GAT-1, a (Na(+)+Cl(−))-coupled gamma-aminobutyric acid transporter from rat brain, impairs net flux but not exchange. J. Biol. Chem. 275, 34106–34113.

Cao, Y., Li, M., Mager, S., Lester, H.A., 1998. Amino acid residues that control pH modulation of transport-associated current in mammalian serotonin transporters. J. Neurosci. 18, 7739–7749.

Chen, N., Reith, M.E., 2002. Structure–function relationships for biogenic amine neurotransmitter transporters. In: Reith, M.E. (Ed.), Neurotransmitter Transporters. Humana Press, Totowa, NJ, pp. 53–109.

Chen, J.G., Rudnick, G., 2000. Permeation and gating residues in serotonin transporter. Proc. Natl. Acad. Sci. U. S. A. 97, 1044–1049.

Chen, J.G., Sachpatzidis, A., Rudnick, G., 1997. The third transmembrane domain of the serotonin transporter contains residues associated with substrate and cocaine binding. J. Biol. Chem. 272, 28321–28327.

Chen, N., Ferrer, J.V., Javitch, J.A., Justice Jr., J.B., 2000. Transport-dependent accessibility of a cytoplasmic loop cysteine in the human dopamine transporter. J. Biol. Chem. 275, 1608–1614.

Dimmic, M.W., Mindell, D.P., Goldstein, R.A., 2000. Modeling evolution at the protein level using an adjustable amino acid fitness model. Pacific Symp. Biocomput., 18–29.

Donnelly, D., Overington, J.P., Ruffle, S.V., Nugent, J.H., Blundell, T.L., 1993. Modeling alpha-helical transmembrane domains: the calculation and use of substitution tables for lipid-facing residues. Protein Sci. 2, 55–70.

Felsenstein, J., 1981. Evolutionary trees from DNA sequences: a maximum likelihood approach. J. Mol. Evol. 17, 368–376.

Ferrer, J.V., Javitch, J.A., 1998. Cocaine alters the accessibility of endogenous cysteines in putative extracellular and intracellular loops of the human dopamine transporter. Proc. Natl. Acad. Sci. U. S. A. 95, 9238–9243.

Forlani, G., Bossi, E., Ghirardelli, R., Giovannardi, S., Binda, F., Bonadiman, L., Ielmini, L., Peres, A., 2001. Mutation K448E in the external loop 5 of rat GABA transporter rGAT1 induces pH sensitivity and alters substrate interactions. J. Physiol. 536, 479–494.

Goldberg, N.R., Beuming, T., Weinstein, H., Javitch, J.A., 2003. A structural context for studying neurotransmitter transporter function, In: Schousboe, A. (Ed.), Strategies in Molecular Neuropharmacology. Humana Press, pp. 213–234.

Golovanevsky, V., Kanner, B.I., 1999. The reactivity of the gamma-aminobutyric acid transporter GAT-1 toward sulfhydryl reagents is conformationally sensitive. Identification of a major target residue. J. Biol. Chem. 274, 23020–23026.

Henry, L.K., Adkins, E.M., Han, Q., Blakely, R.D., 2003. Serotonin and cocaine-sensitive inactivation of human serotonin transporters by methanethiosulfonates targeted to transmembrane domain 1. J. Biol. Chem.

Hilgemann, D.W., Lu, C.C., 1999. GAT1 (GABA:Na^+:Cl^-) cotransport function. Database reconstruction with an alternating access model. J. Gen. Physiol. 114, 459–475.

Huelsenbeck, J.P., Ronquist, F., 2001. MrBayes: Bayesian inference of phylogenetic trees. Bioinformatics 17, 754–755.

Kawashima, S., Ogata, H., Kanehisa, M., 1999. AAindex: amino acid index database. Nucleic Acid Res. 27, 368–369.

Keshet, G.I., Bendahan, A., Su, H., Mager, S., Lester, H.A., Kanner, B.I., 1995. Glutamate-101 is critical for the function of the sodium and chloride-coupled GABA transporter GAT-1. FEBS Lett. 371, 39–42.

Koshi, J.M., Goldstein, R.A., 1998. Models of natural mutations including site heterogeneity. Proteins: Struct., Funct., Genet. 32, 289–295.

Koshi, J.M., Mindell, D.P., Goldstein, R.A., 1999. Using physical-chemistry-based substitution models in phylogenetic analyses of HIV-1 subtypes. Mol. Biol. Evol. 16, 173–179.

Krogh, A., Larsson, B., von Heijne, G., Sonnhammer, E.L., 2001. Predicting transmembrane protein topology with a hidden Markov model: application to complete genomes. J. Mol. Biol. 305, 567–580.

Kyte, J., Doolittle, R.F., 1982. A simple method for displaying the hydropathic character of a protein. J. Mol. Biol. 157, 105–132.

Loland, C.J., Norregaard, L., Litman, T., Gether, U., 2002. Generation of an activating Zn(2+) switch in the dopamine transporter: mutation of an intracellular tyrosine constitutively alters the conformational equilibrium of the transport cycle. Proc. Natl. Acad. Sci. U. S. A. 99, 1683–1688.

Lopez-Corcuera, B., Nunez, E., Martinez-Maza, R., Geerlings, A., Aragon, C., 2001. Substrate-induced conformational changes of extracellular loop 1 in the glycine transporter GLYT2. J. Biol. Chem. 276, 43463–43470.

MacAulay, N., Meinild, A.K., Zeuthen, T., Gether, U., 2003. Residues in the extracellular loop 4 are critical for maintaining the conformational equilibrium of the gamma -aminobutyric acid (GABA) transporter-1. J. Biol. Chem.

Ni, Y.G., Chen, J.G., Androutsellis-Theotokis, A., Huang, C.J., Moczydlowski, E., Rudnick, G., 2001. A lithium-induced conformational change in serotonin transporter alters cocaine binding, ion conductance, and reactivity of Cys-109. J. Biol. Chem. 276, 30942–30947.

Norregaard, L., Gether, U., 2001. The monoamine neurotransmitter transporters: structure, conformational changes and molecular gating. Curr. Opin. Drug Discov. Dev. 4, 591–601.

Norregaard, L., Loland, C.J., Gether, U., 2003. Evidence for distinct sodium, dopamine and cocaine dependent conformational changes in transmembrane segments 7 and 8 of the dopamine transporter. J. Biol. Chem.

Pollock, D.D., Taylor, W.R., 1997. Effectiveness of correlation analysis in identifying protein residues undergoing correlated evolution. Protein Eng. 10, 647–657.

Reith, M.E., Berfield, J.L., Wang, L.C., Ferrer, J.V., Javitch, J.A., 2001. The uptake inhibitors cocaine and benztropine differentially alter the conformation of the human dopamine transporter. J. Biol. Chem. 276, 29012–29018.

Rost, B., Casadio, R., Fariselli, P., Sander, C., 1995. Transmembrane helices predicted at 95% accuracy. Protein Sci. 4, 521–533.

Saier Jr., M.H., 1999. A functional-phylogenetic system for the classification of transport proteins. J. Cell. Biochem. Suppl. 32–33, 84–94.

Shi, L., Simpson, M.M., Ballesteros, J.A., Javitch, J.A., 2001. The first transmembrane segment of the dopamine D2 receptor: accessibility in the binding-site crevice and position in the transmembrane bundle. Biochemistry 40, 12339–12348.

Smicun, Y., Campbell, S.D., Chen, M.A., Gu, H., Rudnick, G., 1999. The role of external loop regions in serotonin transport. Loop scanning mutagenesis of the serotonin transporter external domain. J. Biol. Chem. 274, 36058–36064.

Soyer, O.S., Dimmic, M.W., Neubig, R.R., Goldstein, R.A., 2002. Using evolutionary methods to study G-protein coupled receptors. Pacific Symp. Biocomput., 625–636.

Soyer, O.S., Dimmic, M.W., Neubig, R.R., Goldstein, R.A., submitted for publication. Evolutionary insights on dimerization in aminergic G-protein coupled receptors: application of a novel hidden site-class model of evolution.

Stephan, M.M., Chen, M.A., Penado, K.M., Rudnick, G., 1997. An extracellular loop region of the serotonin transporter may be involved in the translocation mechanism. Biochemistry 36, 1322–1328.

Tamura, S., Nelson, H., Tamura, A., Nelson, N., 1995. Short external loops as potential substrate binding site of gamma-aminobutyric acid transporters. J. Biol. Chem. 270, 28712–28715.

Visiers, I., Ballesteros, J.A., Weinstein, H., 2002. Computational methods for the construction and analysis of three dimensional representations of GPCR structures and mechanisms. Methods Enzymol. 343, 329–371.

Yang, Z., 1993. Maximum-likelihood estimation of phylogeny from DNA sequences when substitution rates differ over sites. Mol. Biol. Evol. 10, 1396–1401.

Yang, Z., Rannala, B., 1997. Bayesian phylogenetic inference using DNA sequences: a Markov chain Monte Carlo method. Mol. Biol. Evol. 14, 717–724.